

CONF-920712-44

Thermal, structural, and fabrication aspects of diamond windows for high power synchrotron x-ray beamlines

Ali M. Khounsary
Advanced Photon Source, Argonne National Laboratory, Argonne, IL 60439,

and

William Phillips
Crystallume, Menlo Park, CA 94025

ANL/XFD/CP--77991

DE93 004194

ABSTRACT

Recent advances in chemical vapor deposition (CVD) technology have made it possible to produce thin free-standing diamond foils that can be used as the window material in high heat load synchrotron beamlines. Numerical simulations suggest that these windows can offer an attractive and at times the only alternative to beryllium windows for use in third generation x-ray synchrotron radiation beamlines. Utilization, design, and fabrication aspects of diamond windows for high heat load x-ray beamlines are discussed, as are the microstructure characteristics bearing on diamond's performance in this role. Analytic and numerical results are also presented to provide a basis for the design and testing of such windows.

1. INTRODUCTION

X-ray windows are often used on the front ends of synchrotron beamlines to isolate the ultra-high vacuum of the storage ring from the downstream environment. The windows are usually made of low-atomic-number materials, such as beryllium, for maximum x-ray transmission. Nonetheless, the intense x-ray beams generated by undulators and wigglers at high-energy storage rings can deposit substantial amounts of localized heat in passing through the commonly used beryllium windows. Although these windows are actively cooled, the temperature and/or stress in a window can become unacceptably high, leading to failure of the window.

One solution to this problem is to reduce the thermal load on the windows by using thermal filters upstream of a beryllium window. Thermal filters are made of thin foils of low-atomic-number materials, which can withstand high temperatures. They may also be cooled radiatively. Foils of pyrolytic graphite are often used for this purpose, although diamond foils may provide a better alternative. Thermal filters will absorb primarily low-energy photons that would otherwise be absorbed in the beryllium window. Figure 1 depicts the absorbed power in two successive 10-mil-thick beryllium windows as the thickness of the upstream carbon filter is increased. The radiation source is the 5-m-long Undulator A at the Advanced Photon Source (APS), with a total power of about 10 kW (see Table I). Figure 1 illustrates two important points. First, as the thickness of the thermal filter(s) is increased, the reduction in the absorbed power in a beryllium window becomes less pronounced. Absorption in the beryllium window will then be primarily due to Compton scattered photons as few photons with energies below 4 keV remain after the beam passes through a few hundred microns of carbon filter. The transmittance curves for diamond and carbon are shown in Fig. 2. Second, as shown in Figure 1, after a few hundred microns of filter, the x-ray beam deposits almost identical amount of heat in each of the two beryllium windows usually used in the window assembly. Therefore, one of the reasons for using a double-beryllium window assembly (in which the first window is expected to take the brunt of the heat load leaving the second one with a much smaller thermal load and thus more durable) vanishes. This will have implications in the design of windows for high heat load beamlines.

The submitted manuscript has been authored by a contractor of the U. S. Government under contract No. W-31-109-ENG-38. Accordingly, the U. S. Government retains a nonexclusive, royalty-free license to publish or reproduce the published form of this contribution, or allow others to do so, for U. S. Government purposes.

REPRODUCTION OF THIS DOCUMENT IS UNLIMITED EP

MASTER

In the calculations reported here, it is conservatively assumed that all the attenuated photons from the beam are absorbed. As such, the absorption values given here may exceed the actual values by as much as thirty percent. This estimate is obtained by varying the self-absorption term in the calculations from zero (all scattered radiation leave the medium) to unity (all scattered radiation is absorbed in the medium).

The total absorbed power (shown in Fig. 1), as well as its spatial distribution in a window, are estimated by simulating the insertion device (ID) spectrum by a bending magnet spectrum of an appropriate characteristic energy. The PHOTON¹ program is used for this purpose. PHOTON gives the absorbed power as well as its distribution in the vertical direction. In the horizontal direction, it has throughout been assumed that the absorption profile is similar to the source profile; the implicit assumption being that the ID beam is horizontally uniform in energy.² This, of course, is not true, since the x-ray beam softens as one moves off-axis in the horizontal direction. In fact, it has recently been shown that the peak absorbed heat flux in a beryllium foil subjected to an ID beam may not be in the central region of the beam footprint but at a horizontally off-axis location.³ This will not significantly affect the present thermal and structural analyses, but will have to be incorporated in refined design analyses. The development of an extension to the PHOTON program, named PHOTON2, to properly account for the vertical as well as the horizontal energy distribution of a wiggler beam and its absorption in media is being completed.⁴

Table I. Parameters for the APS Undulator A*

Parameter	Value
Storage ring energy [GeV]	7.0
Storage ring current [mA]	100
Period length [cm]	3.1
Device length [m]	5.0
Number of periods	160
Max. magnetic field B ₀ [T]	0.80
Characteristic energy E _c [keV]	26.0
1/γ [mrad]	0.073
Maximum deflection parameter, K	2.51
K/γ [mrad]	0.183
Total power [kW]	10.0
Peak power density [kW/mrad ²]	333
Peak heat flux @24 m [kW/mm ²]	0.58

*Current Undulator A parameters are slightly different.

2. AN ANALYTICAL MODEL OF A COOLED WINDOW

In order to estimate the temperature and stress in the thin foil window subjected to an incident x-ray beam, a simple one-dimensional model is devised. As shown in Fig. 3, the foil is represented by an infinitely long thin plate of thickness t and width w (corresponding to the vertical opening size of a window). The absorbed heat in the foil is approximated by an infinitely long line-source, which is uniformly distributed throughout the thickness of the foil. The window is convectively edge-cooled along its length, as illustrated in Fig. 3.

Assuming a linear heat flux of q' [W/cm] for the absorbed radiation in the thin foil, the steady state temperature profile in the foil is given by⁵ (see Fig. 3):

$$T(x) - T_{\infty} = \frac{q'}{2t} \left[\frac{(w - 2x)}{2k} + \frac{1}{h} \right] \quad (1)$$

where k [W/cm-K] is the thermal conductivity of the foil, T [°C] is the temperature, x [cm] is the lateral distance measured from the center of the foil, t [cm] is the thickness of the foil, h [W/cm²-K] is the heat-transfer coefficient, and T_∞ [°C] is the temperature of the coolant.

The overall maximum temperature rise is

$$\Delta T_{\max} = T(0) - T_\infty = \frac{q'}{2t} \left[\frac{w}{2k} + \frac{1}{h} \right], \quad (1a)$$

while the maximum temperature rise in the foil is given by

$$\Delta T_{\text{foil}} = T(0) - T(w/2) = \frac{q'}{2t} \left[\frac{w}{2k} \right]. \quad (1b)$$

Assuming an initial foil temperature of T_∞ , the strain ϵ in the (simply supported) heated foil is⁵

$$\epsilon = \frac{q' \alpha}{2t} \left\{ \frac{w}{4k} + \frac{1}{h} \right\}, \quad (2)$$

where α [K⁻¹] is the thermal expansion coefficient which is assumed to be independent of temperature. The stress σ [N/cm²] that would result in the foil if it were laterally constrained is

$$\sigma = -\epsilon E = -\frac{q'}{2t} \left[\frac{w}{4k} + \frac{1}{h} \right] \alpha E. \quad (3)$$

The negative sign emphasizes that the stress is compressive.

The width of a beryllium foil (which is mounted on a cooled, conductive platform) is somewhat larger than the opening size of the window, by about 1 cm or so. Thus, from a cooling point of view, there is a fin effect that the above analytical model ignores. In fact, cooling is substantially better than the assumed convective edge-cooling. A better approximation in this case may be obtained by assuming that the window edge is maintained at the coolant temperature. Then Eqs. 1a and 1b become identical, and the temperature and stress in the window are, respectively, given by

$$T(x) - T_\infty = \frac{q'}{2t} \left[\frac{(w - 2x)}{2k} \right], \quad (4)$$

$$\sigma = -\frac{q' w}{8tk} \alpha E. \quad (5)$$

As an example, Eqs. 4 and 5 can be used to estimate the maximum allowable temperature and stress in a diamond and a beryllium foil. For beryllium, the absorbed power is limited by the allowable

stress. Assuming a stress level equivalent to the yield strength of beryllium (~350 MPa) and using data in Table II, the maximum allowable linear flux q' in a 250 μm -thick, 1.05 cm-wide beryllium window is

$$q' = -\frac{8tk\sigma}{w\alpha E} = 35 \text{ W / cm}, \quad (6)$$

and the maximum temperature rise in the window will be

$$\Delta T_{\text{max}} = \frac{q' w}{4tk} = 182^\circ \text{C}, \quad (7)$$

so that for a coolant temperature of 32°C, the maximum temperature in the beryllium window will be about 214°C (these estimates are based on *bulk* beryllium properties; foil properties may vary significantly from the bulk values.)

Table II. Properties of Diamond and Beryllium at Room Temperature

Property	Diamond	Beryllium
Atomic Number, Z	6	4
Density (g/cm^3)	3.5	1.85
Thermal Conductivity (W/cm-K)	21*	2.0
Thermal Expansion Coefficient ($\text{K}^{-1} \times 10^{-6}$)	0.8	12
Specific Heat (J/Kg-K)	520	1850
Thermal Diffusivity (cm^2/s)	<11.5	5.7
Young's Modulus (GPa)	1,050	320
Poisson's Ratio	0.1-0.29	0.02-0.08
Melting Point (°C)	NA	1280
Tensile Strength (GPa)	>3	0.080-0.550
Yield Strength (MPa)	NA	70-480

*Single-crystal value. See Figure 10 for polycrystalline CVD diamond film values.

For diamond, the absorbed power is limited by its oxidation temperature of about 600 °C (it is understood, however, that the window may operate at higher temperatures in a high vacuum environment). Then from Eqs. 1b and 5, the maximum allowable linear heat flux and stress in a 50 μm -thick, 1.05 cm-wide diamond window will be 92 W/cm and 715 MPa, respectively. Properties of single-crystal diamond at an average temperature of 350 °C are evaluated and used in these calculations. When the thermal conductivity expected for a currently available 50 μm polycrystalline diamond foil is substituted, the maximum heat flux may be considerably reduced (see Section 5).

Detailed finite element analyses discussed next show a maximum allowable temperature of about 180 °C (cf. analytic models 214 °C) in the beryllium window and a compressive stress of about 1100 MPa (cf. analytic models 715 MPa) for the diamond window. Recent synchrotron thermal tests at the Photon Factory in Japan on a 300 μm Be window show that the window fails when the temperature difference across the window exceeds about 200°C.⁶

The simple analytical expressions derived above must be used with caution in estimating the temperature and stress levels in the windows. These results can be used, however, to establish thermal and structural figures of merit for various window-foil materials. The absorption of the x-ray beam in diamond and beryllium is assumed to be roughly proportional to the square of their atomic numbers (Z) of 6 and 4, respectively. This gives 2.25 times more absorption in diamond than in beryllium. More detailed

calculations (discussed later and shown in Fig. 7) indicate that, for the APS Undulator A beam, this energy-dependent figure is between 5 and 2. Defining a thermal figure of merit as proportional to the inverse of the maximum temperature rise ΔT_{\max} (Eq. 1b), and replacing q' by Z^2 results in $(\Delta T_{\max})^{-1} \sim k/Z^2$. Similarly, a structural figure of merit can be defined as being proportional to the inverse of the thermal stress in the foil. From Eq. 5, one obtains the relationship $\sigma^{-1} \sim k/(Z^2 \alpha E)$. Using the material properties given in Table II, the relative figures of merit for beryllium and diamond are obtained and listed in Table III. For CVD polycrystalline diamond films, a conservatively low thermal conductivity of 7 W/cm-K is assumed.

Table III. Figures of Merit for Diamond and Beryllium

Figure of Merit	Relationship	Beryllium	Diamond Crystal	Diamond CVD Film
Thermal (ΔT^{-1})	k/Z^2	1	4	1.3
Structural (σ^{-1})	$k/(Z^2 \alpha E)$	1	20	7

3. COMPUTATIONAL ANALYSES OF BERYLLIUM AND DIAMOND WINDOWS

In order to provide a more reliable simulation of the window performance under the realistic heating condition of an incident beam, a finite element model is set up and used for analyses. The model allows an accurate description of the window configuration, the spatial variation of the absorbed heat flux, the thermal and structural boundary conditions, and temperature dependency of the physical properties of the window material. The window configuration used for the analysis is sketched in Fig. 4. Due to symmetry, one quadrant of the window is shown and modeled. The diamond or beryllium foil is mounted on a back-cooled copper block. The window opening is 1.05 cm, which corresponds to a $6/\gamma$ opening angle at 24 m from the source ($1/\gamma$ is the intrinsic opening angle of the x-ray beam, and for the APS it has a value of 73 μ rad). The horizontal extent of the APS Undulator A beam at the window is about 1 cm. The much larger horizontal dimension of the window is to allow it to be used on the wiggler beamlines as well.

The main objective here is to determine the minimum amount of upstream thermal filter necessary to reduce the absorbed power in a window to an acceptable level. One way to do this is to assume a certain amount of filter(s) upstream of the window, obtain the maximum temperature and stress in the window, compare these with the applicable limits, and repeat this process until the minimum amount of filter necessary is obtained. Alternatively, maps of the absorbed power, absorbed-power profile, temperature, and stress can be developed from which the filter requirement can be determined.²

For the purpose of the present study, a typical absorbed power profile in the window is assumed: it has Gaussian profile in the vertical direction (along the width of the window) with a full width at half maximum (FWHM) of 0.6 cm, and a parabolic profile in the horizontal direction (along the length of the window) similar to the incident beam on-axis horizontal-power profile. It must be noted that the vertical FWHM of the absorbed power varies with the thickness of the upstream thermal filters, and the 0.6 cm value used here is only a representative value.

Figures 5 and 6 show, respectively, the maximum temperature and the maximum (equivalent) stress as a function of the total absorbed power in one beryllium window and in two diamond windows. The beryllium window is 250 μ m-thick, while the diamond windows are 50 μ m and 100 μ m-thick. As stated earlier, for the beryllium window the stress is limited to some 350 MPa, while for the diamond

window the maximum temperature must not exceed 600°C. These conditions, as shown in Figs. 5 and 6, limit the absorbed power in the beryllium window to about 40 W, and in the 50 and 100 μm diamond windows to about 150 and 300 W, respectively. From Fig. 1, it can be seen that several millimeters of carbon filter are needed to reduce the absorbed power in the beryllium window to about 40 W. This much filter, as Fig. 2 indicates, will attenuate the 8 keV photons by about three orders of magnitude and the 12 keV photons by about one. Thus, this window/filter arrangement is not acceptable.

Turning now to the diamond alternative and considering the 50 μm-thick window (which can accept about 150 W of power), it is noted that, if exposed directly to the Undulator A beam, it will absorb some 900 W of heat (Fig. 7). Thus, thermal filters are necessary even in this case. Since for a given compound absorption is proportional to density, the amount of *carbon* filter needed can be estimated by considering the absorption equation for *diamond* obtained by a curve fit through the computed data points shown in Fig. 7, that is,

$$P_{\text{abs,D}} [\text{W}] \approx 190t^{0.4} [\mu\text{m}]. \quad (8)$$

Differentiating Eq. 8 and using the 150 W allowable absorbed power in the 50-μm-thick diamond window, one obtains

$$\frac{dP_{\text{abs,D}}}{dt} \equiv \frac{150 \text{ W}}{50\mu} \approx 76t^{-0.6}, \quad (9)$$

which gives the total diamond-equivalent thickness of upstream filter as

$$t \approx 215 \mu\text{m}. \quad (10)$$

This corresponds to about 360 μm of carbon ($\rho=2.1 \text{ g/cm}^3$). From Fig. 2, it is now seen that the transmission of the 8 keV photons through this much carbon filter is over 30% and is still higher for the 12 keV photons. This clearly demonstrates the advantage of diamond windows (the chemical inertness of a diamond window is another advantage when compared to a beryllium window).

A moderate increase or decrease in the thickness of the diamond window will not have a significant impact on its temperature or stress, since the absorbed power is similarly increased or decreased. Using thinner, yet vacuum-tight diamond windows, however, remains a possibility since it would allow a somewhat higher transmission. With beryllium, the window sizes used in the present application require a thickness of at least 5 mil (127 μm) to ensure vacuum integrity.

It should be noted that in the present analyses, an important parameter, namely the window opening, was fixed at a value of 1.05 cm ($=6/\gamma$ at 24 m from the source). As seen from the analytic solution (e.g., Eqs. 8 and 10) and verified with more accurate analyses, reducing the window opening will correspondingly reduce the temperature and stress levels in the windows. The conservative window opening of $6/\gamma$ used here is consistent with the present designs at various synchrotron facilities and with the concerns with beam missteering and stability. The high heat load of the APS undulator beamlines, however, has provided a compelling reason to carefully examine the window size requirements imposed by the stability of the beam. It has been shown,⁷ for example, that for the 2.5m-long APS Undulator A beamline it is possible to use a beryllium window with an opening size of 0.7 cm (corresponding to an opening angle of $4/\gamma$ at the source) with only a moderate amount of upstream carbon filter. And with an

opening size of 0.35 cm (corresponding to an opening angle of $2/\gamma$ at the source), a beryllium window can be used on the 5m-long APS undulator beamline. But even for smaller window openings, diamond windows remain superior since they can be used with a lower amount of thermal filters upstream resulting in higher photon transmission through the filter-window assemblies. In the computations here, properties of single crystal diamond are used. Corresponding values for polycrystalline diamond developed by the CVD process will be somewhat different, as discussed in the following sections.

Finally, we note that the preceding numerical results are based on an elastic analysis of windows; buckling and plastic analyses should be carried out and correlated with experimental results in order to provide reliable guidelines for high heat load window design. The necessity of experimental verification cannot be over-emphasized, for the uncertainty inherent in these latter calculations, unless experimentally confined, requires unacceptably large safety margins for the present application.

4. GROWTH OF DIAMOND FILMS FOR WINDOWS

The diamond films envisioned for the synchrotron window application are the product of advances in CVD diamond technology that have been taking place at an accelerating pace over the last fifteen years. To fabricate windows, plasma-enhanced CVD is used to deposit the diamond films on a suitable substrate, such as silicon or molybdenum. The substrate is then etched away entirely or in part, to leave a free-standing diamond membrane. Membrane thickness can vary from a fraction of a micron to a millimeter or more.

Diamond CVD deposition chemistry is shown schematically in Figure 8. Hydrogen-hydrocarbon mixtures are dissociated by the plasma and various short-lived excited species are formed. One of these, atomic hydrogen, is critical for diamond deposition. The identity of the carbon species responsible for diamond deposition is not firmly established, although methyl radicals (CH_3^0) and acetylene (C_2H_2) are thought to be important. Substrate temperatures for diamond deposition usually range between 700 °C - 950 °C, with a broad optimum at ~800°C. Growth rates in the range 1 to 15 microns per hour are typical. Temperatures as low as 350 °C can be employed, but they generally incur greatly reduced deposition rates.

Diamond films can be synthesized using a wide variety of plasma-excitation techniques, each of which has its unique set of advantages and disadvantages. Diamond films can be formed using heated filaments, DC glow discharges, fuel/oxidizer combustion flames, plasma torches, and microwave discharges. Diamond films comprised of near-single crystal diamond⁸, for example, may be a possible candidate for windows and other x-ray applications. Choice of specific deposition technology, parameters, and substrate materials largely determines the properties of the material deposited, and there is therefore no single "best" deposition method.

5. GRAIN STRUCTURE OF DIAMOND FILMS

Diamond film growth starts with the formation of isolated, randomly oriented nuclei on the surface of the substrate. It is usual to have to seed a substrate by rubbing it with diamond powder to get nucleation to occur, although some growth methods do not require this step. The individual nuclei grow until they coalesce, forming a continuous film. The initial grain size of the film is therefore determined primarily by the nucleation density (see Fig. 9). The film continues to grow with a columnar grain structure. Grain size increases because grains with faster-growing orientations overwhelm those with slower growing orientations. Figure 9 is an edge view of a diamond film, illustrating the evolution of grain size with thickness. Diamond films are usually described according to the grain size as measured at the top surface of the film.

From the preceding analysis, it is seen that the advantage of the diamond film, in the main, results from its high thermal conductivity coupled with a low thermal coefficient of expansion and a high Young's modulus. It is, therefore, important to examine the properties of polycrystalline films in comparison with single crystal diamond.

Recent work by Graebner, Lin, and Kamlott (at AT&T Bell Labs) and Herb and Gardinier (at Crystallume) demonstrated⁹ that extraordinarily high thermal conductivities, even exceeding published values for Type 2A natural diamond, can be achieved in CVD films. Thermal conductivity of films is shown to be a function of grain size and is lower for smaller grain sizes. The conductivity of a film in the direction parallel to the substrate is an average over all grain sizes in the film thickness and is therefore lower for thinner films comprised primarily of small diamond grains.

The situation is summarized in Figure 10 (taken from Reference 9). From the lower curve, we estimate a thermal conductivity of about 7 W/cm-C for a 50 μm -thick film, compared with 21 W/cm-C for single crystals. The top curve shows the *local* conductivity as a function of distance from the bottom of the film. If we could produce films with grain structure similar to the top portion of the few-hundred micron thick films (Fig. 10), it would have a thermal conductivity closely matching or exceeding that of single-crystal value.

In principle, this can be accomplished by growing a thick film and polishing away the bottom portion. This is not a practical window fabrication procedure, but demonstrates that process development leading to elimination of smaller grains could lead to high conductivity thin diamond films. Such process development would take the form of increasing the initial grain size of the films, eliminating as much as possible of the low thermal conductivity material.

Young's modulus E is another parameter for which we can anticipate a departure from the single crystal value. Data available for CVD films is minimal, but some bulge-test measurements¹⁰ have been made on diamond membranes produced for x-ray lithography masks having submicron grain size. Bulge measurements do not lead to E directly, but to a reduced modulus $E/(1-\nu)$ in which ν is Poisson's ratio. Figure 11 shows data for several films. While there is a departure from the anticipated single crystal value of $E/(1-\nu)$, about 1300 MPa for the small grain films measured, there is a clear trend toward higher values for larger grain sizes. Since grain sizes of about 5 μm are anticipated for diamond synchrotron windows, it appears justified from Figure 11 to assume the single crystal value of E for 50 μm and thicker windows.

The thermal coefficient of expansion (TCE) for CVD films has not been measured by us, but it can be expected to be an average of the single crystal TCE and the TCE representative of the intergranular-graphitic material. Since the intergranular material represents only a fraction of a percent of the total volume of CVD diamond films, its influence on the average TCE will be minimal. Therefore, the TCE of foils can be expected to be close to the single crystal.

In summary, the thermal conductivity of CVD films in the 50-100 μm thickness range can differ significantly from single crystal thermal conductivity, while the Young's modulus and thermal expansion coefficients will be approximately the same as the single-crystal values.

Even with a lower thermal conductivity, a 50 μm CVD diamond window may be significantly better than a beryllium window. The last column of Table III shows the Figures of Merit based on the thermal conductivity of commonly available CVD films. As indicated earlier, with further development of the diamond deposition process, diamond film thermal properties may approach those of single crystal. In any case, the fortuitous combination of high thermal conductivity, high Young's modulus, low thermal expansion coefficient, and chemical inertness, make diamond an attractive material for x-ray window applications.

6. PRACTICAL ASPECTS OF WINDOW MANUFACTURE

The first commercially available CVD diamond product was the soft x-ray windows¹¹ manufactured by Crystallume, primarily for use in energy dispersive x-ray spectroscopy (EDS). This window, shown in Figure 12, consists of a 0.4 μm -thick diamond film supported by a silicon grid structure. The windows are used at one atmosphere pressure and are tested above three atmospheres. Synchrotron windows will be sufficiently thick and do not need a support grid. The films could be grown by several of the techniques mentioned earlier, but microwave growth seems the best all-around choice from the standpoint of thickness uniformity, growth rate, and control of microstructural properties.

Brazing techniques developed for single crystal diamond¹² have been found to be applicable to CVD diamond films. CVD films can be soldered or brazed by a variety of means. They can be metallized effectively with titanium-gold or chrome-gold metallization systems, and subsequently soldered to the support using a gold solder. Alternatively, they can be brazed directly with a number of commonly used ceramic brazes. Those containing transition metals are found to provide the best wetting of the diamond. A window fabrication procedure using a high temperature brazing approach will have to take into account the thermal expansion mismatch between diamond and metals such as copper.

Brazeless window construction can be realized if the substrate upon which the film is grown is utilized as part of the support structure as is the case in the EDS windows. In this case, the window, including its silicon support structure, is mounted so that one surface of the diamond film can be cooled by direct water impingement. This construction has the additional advantage of eliminating the thermal resistance of the braze material between the diamond and the cooled support structure.

7. CONCLUDING REMARKS

Although the superior thermo-physical properties of diamond make diamond windows an attractive and at times the only option for high heat flux synchrotron x-ray beamlines, a number of issues remain unresolved. First is the question of radiation damage and stability of diamond foils and possible degradation of their mechanical properties. In this regard, limited tests¹³⁻¹⁵ on CVD diamond membranes for use in x-ray lithography show no noticeable degradation for x-ray exposures of several MJ/cm^2 . Nevertheless, this issue, and particularly long-term exposure effects, must be further investigated. A 50 μm diamond window on the APS undulator beamline, for example, must survive several hundred MJ/cm^2 of radiation exposure. Scattering effects from the CVD polycrystalline films must be evaluated. Other deposition, fabrication, and testing issues remain, which, however, are within the scope of ongoing research and development activity in the synthetic diamond community.

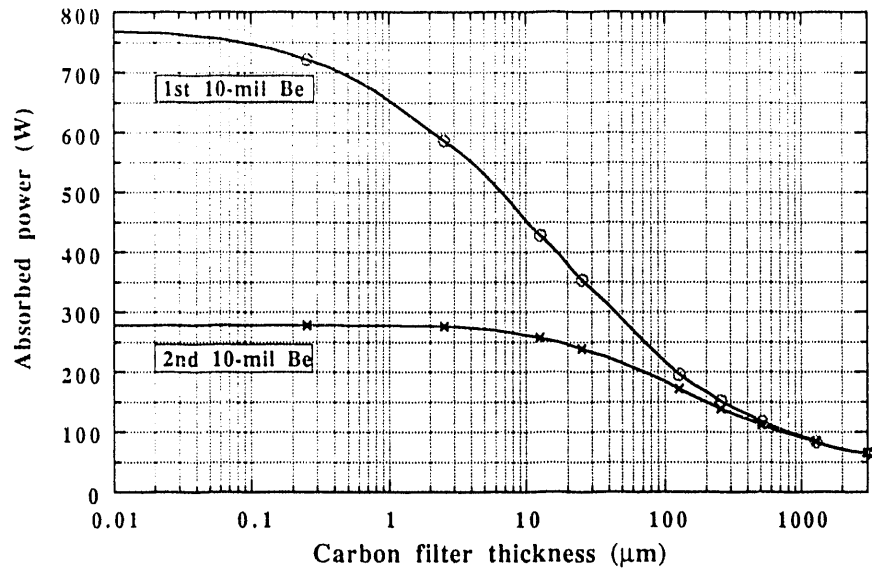


Figure 1. The absorbed power of the 5m-long APS Undulator A beam in two successive beryllium foils as a function of the total thickness of the upstream carbon filter(s). The thickness of each beryllium foil is 10 mils (254 μm).

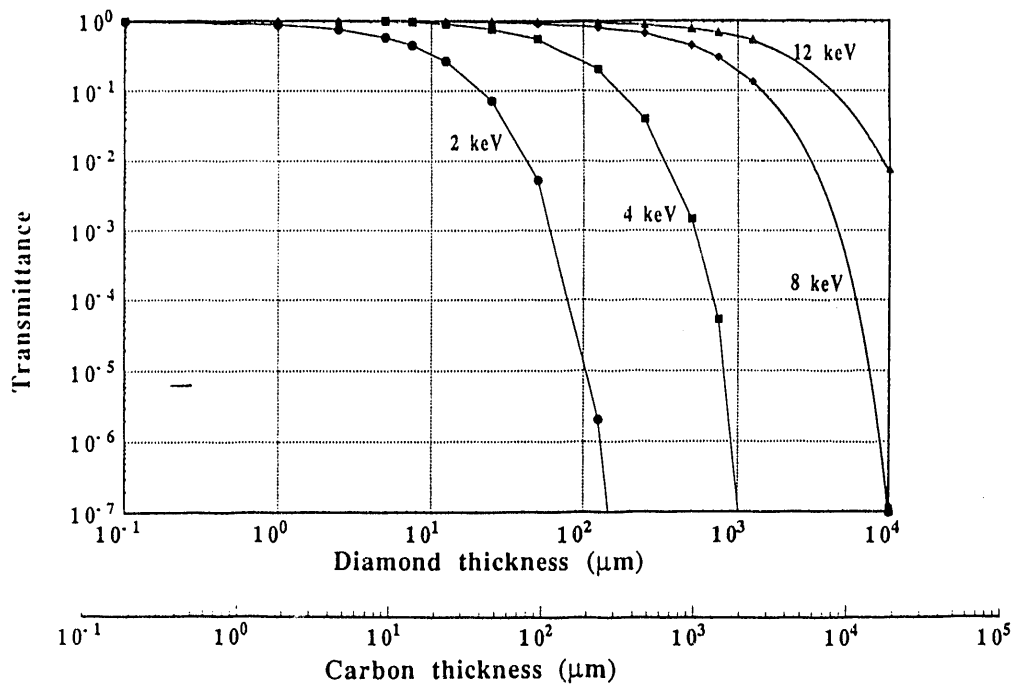


Figure 2. Transmittance of photons of various energies through diamond ($\rho=3.5\text{g/cm}^3$) and carbon ($\rho=2.1\text{g/cm}^3$) foils.

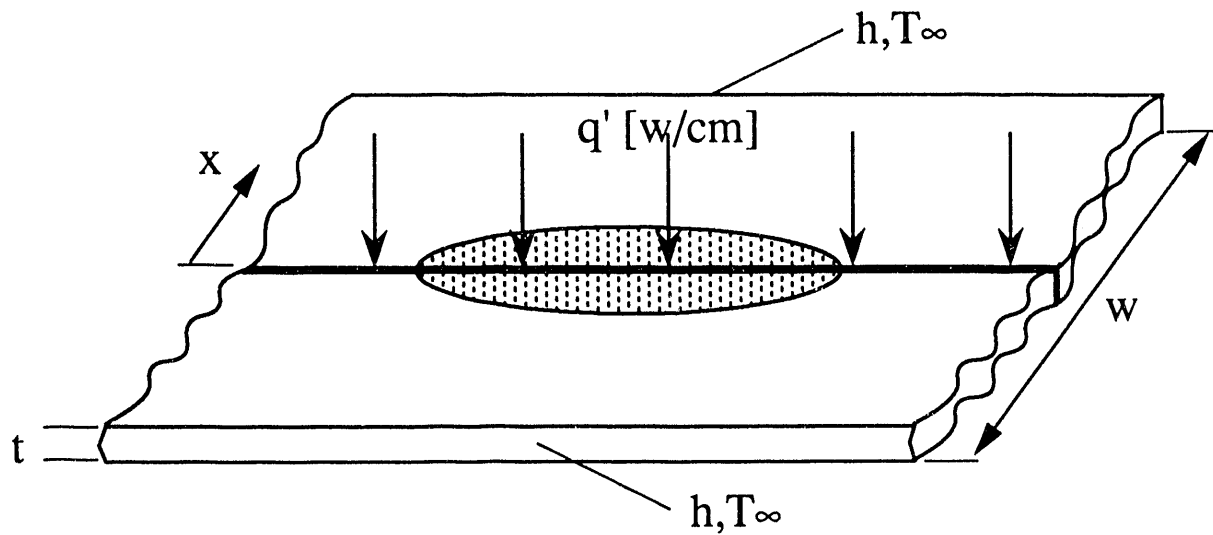


Figure 3. A sketch of the model foil used to develop a simple analytical solution for temperature and stress in a window. The thin, infinitely long plate of width w (equal to the opening size of the window) is subjected to a line heat source of strength q' [W/cm] deposited uniformly throughout its thickness. The plate is convectively edge-cooled along its length. The shaded region is a sketch of a typical beam power footprint.

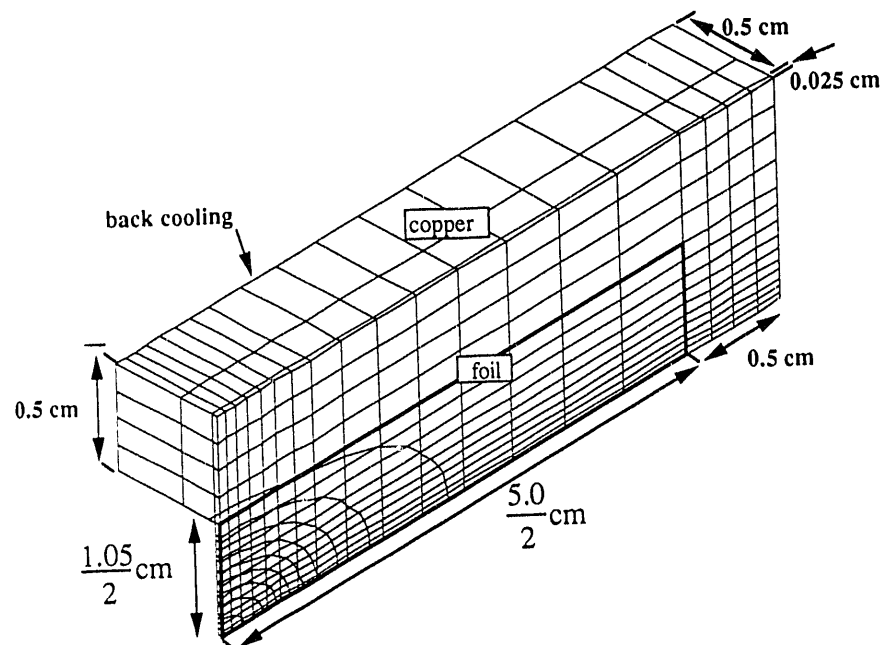


Figure 4. A typical model used in the finite element analysis of the windows. Due to symmetry, only one-quarter of the window is shown here and modeled. The window opening is shown in heavy lines. Also shown are typical temperature contours.

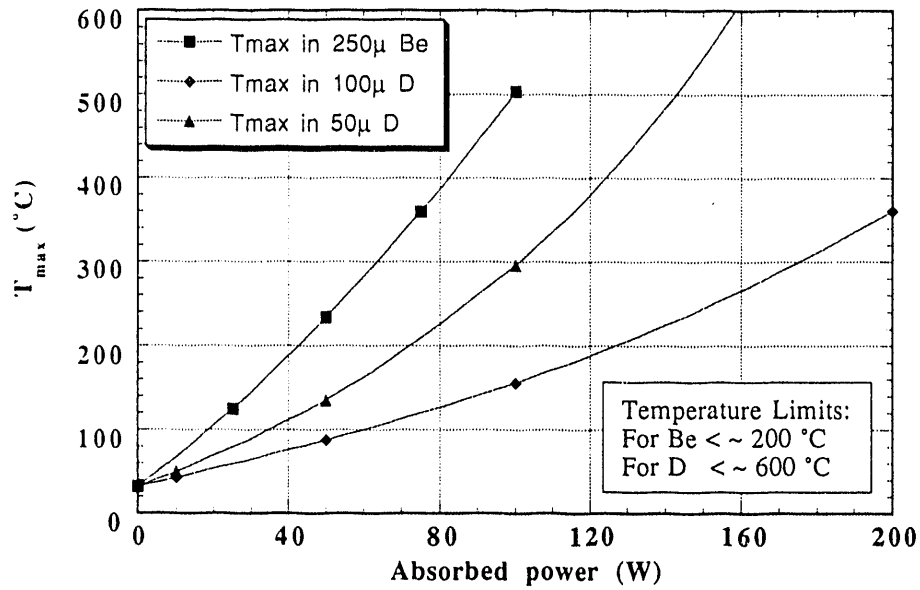


Figure 5. Maximum temperature in a one-beryllium and two-diamond window as a function of the absorbed power. The absorbed power has a vertical Gaussian profile (FWHM = 0.6 cm) and a horizontal parabolic profile (about 1 cm in extent) similar to that of APS Undulator A beam. Window opening is 1.05 cm ($=6/\gamma$).

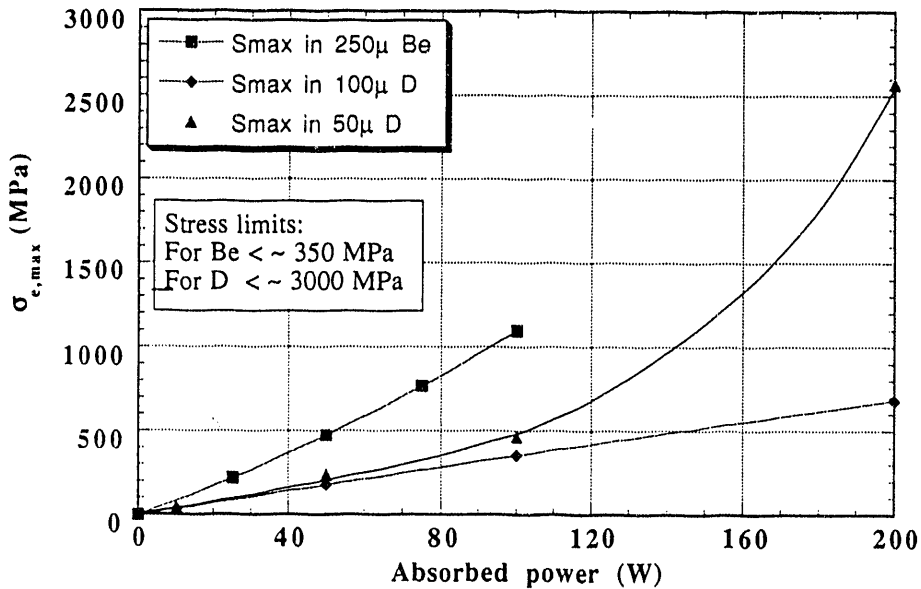


Figure 6. Same as Fig. 5, but instead of the maximum temperature, the maximum stress is shown here.

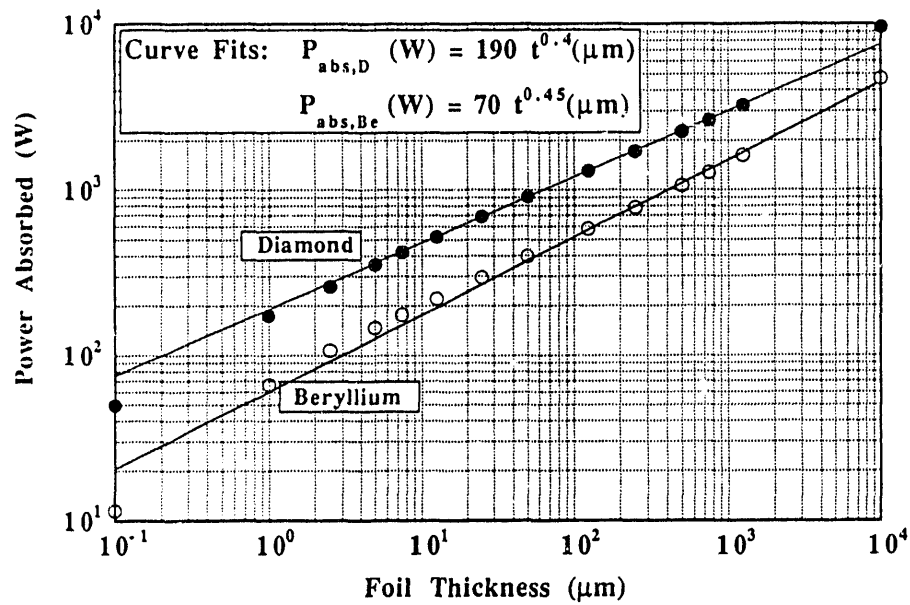


Figure 7. Absorption of the x-ray beam from the 5 m-long APS Undulator A in beryllium and diamond foils. Also shown are the curve fits through the data points.

Diamond CVD Process

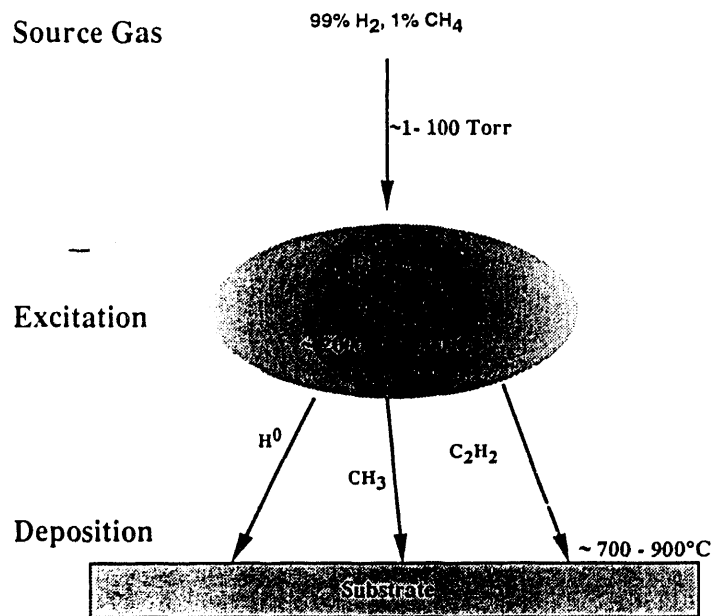


Figure 8. Schematic representation of CVD diamond deposition chemistry.

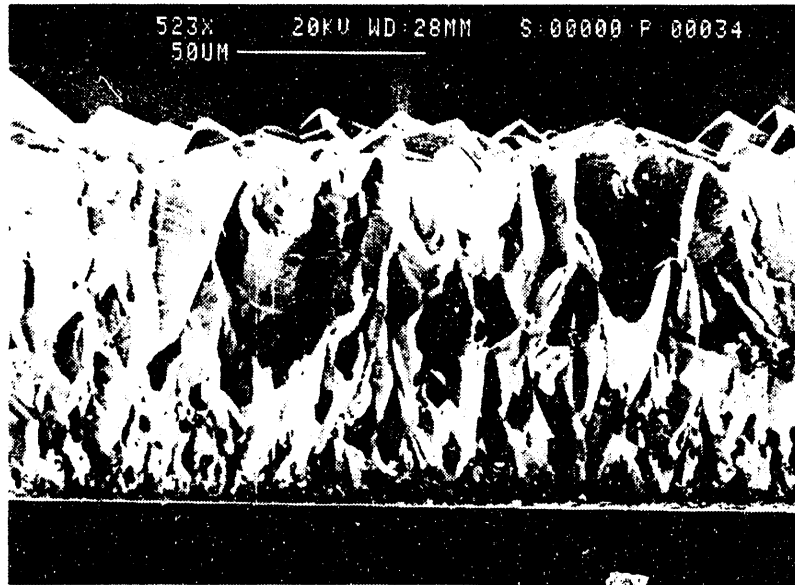


Figure 9. Edge view of CVD diamond film illustrating the evolution of grain size with film thickness.

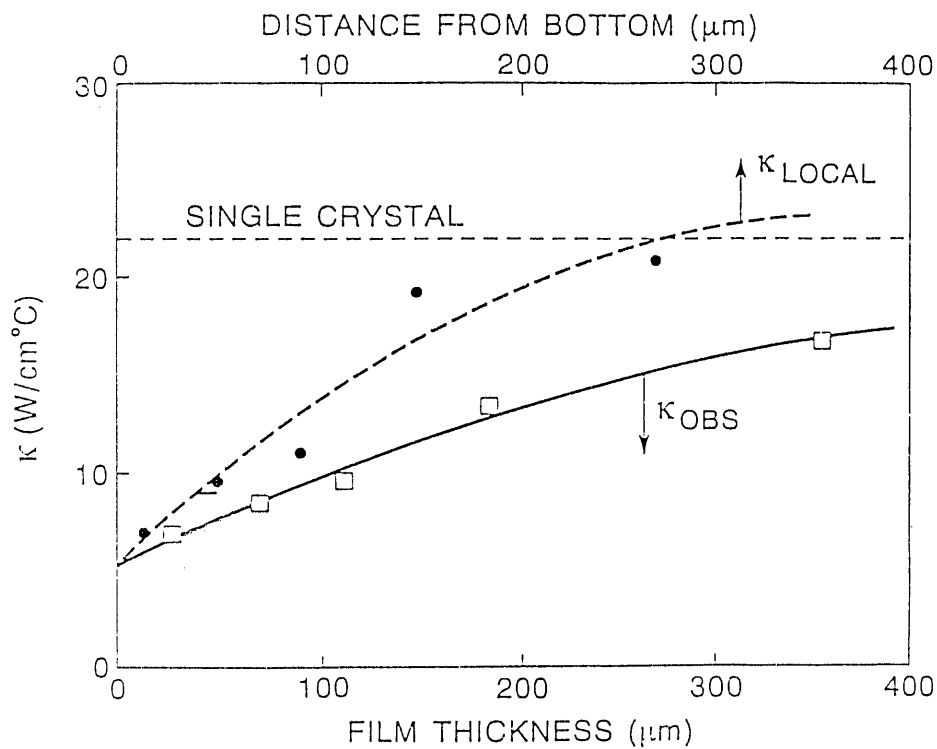


Figure 10. Solid curve: Lateral thermal conductivity of diamond films measured as a function of film thickness. Dashed curve: Local lateral thermal conductivity as a function of the distance from the bottom of the film (Courtesy Graebner et. al.⁹).

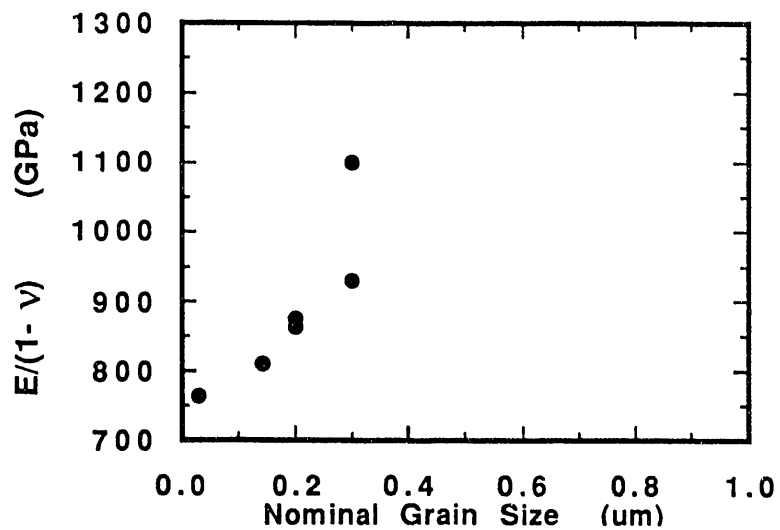


Figure 11. "Membrane" modulus $E/(1-\nu)$ of various membranes as a function of grain size. Extrapolation through the points suggests that for films with grain sizes above $1 \mu\text{m}$ the membrane modulus and the elastic modulus E will be close to the single crystal values.

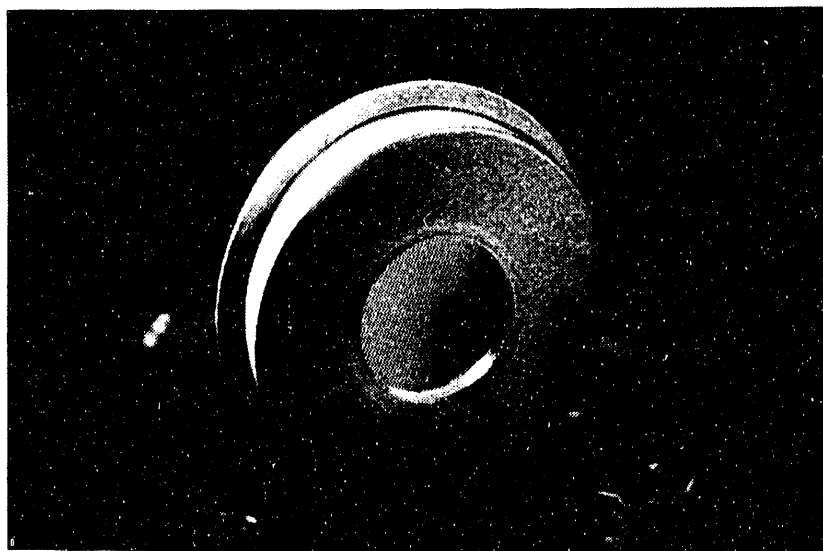


Figure 12. Photograph of an x-ray window manufactured by Crystallume. The unobstructed aperture of this window is 6 mm.

8. ACKNOWLEDGMENTS

This work was supported in part by the U. S. Department of Energy BES Materials Science under Contract No. W-31-109-ENG-38. We would like to thank Mr. M. Moreno for his contributions in obtaining the information presented in Figure 11, and Dr. S. Picologlou for editing this manuscript.

9. REFERENCES

1. D. Chapman, N. Gmuer, N. Lazarz, and W. Thomlinson, *Nucl. Instrum. and Meth.* **A266**, 191-194 (1988).
2. A. M. Khounsary, P. J. Viccaro, and T. M. Kuzay, *SPIE Proceedings* **1345**, 42-54 (1990).
3. R. J. Dejus, A. M. Khounsary, D. A. Brown, and P. J. Viccaro, "Calculation of wiggler spectrum and its absorption in media," *Nucl. Instrum. Meth.* **A319**, 207-212 (1992).
4. A.M. Khounsary, R.J. Dejus, D.A. Brown, P.J. Viccaro, and T.M. Kuzay, To be submitted as a Light Source Note, Advanced Photon Source, Argonne National Laboratory (1992).
5. A.M. Khounsary and T.M. Kuzay, "On diamond windows for high power synchrotron x-ray beams," *Nucl. Instrum. Meth.* **A319**, 233-239 (1992).
6. S. Asaoka, H. Maezawa, Y. Kamiya, and M. Yanagihara, "Experiment on direct irradiation of a beryllium window by undulator radiation," *Rev. Sci. Instrum.* **63(1)**, 473-476 (1992).
7. A.M. Khounsary, "Window and filter assemblies for the APS beamlines," Unpublished information, September 30, 1991.
8. R. Pryor, Private Communication, 1992.
9. J.E. Graebner, S. Lin, G.W. Kammlott, J.A. Herb and C.F. Gardinier, "Unusually High Thermal Conductivity in Diamond Films," *Appl. Phys. Lett.* **60(13)**, 1576-1578 (1992).
10. E.I. Bromley, J.N. Randall, D.C. Flanders, and R.W. Mountain, "A technique for the determination of stress in thin films," *J. Vac. Sci. Technol.* **B 1 (4)**, 1364 (1983).
11. D.A. Fischer and W. Phillips, "Soft x-ray transmission of thin film diamond: Applications to detectors and high pressure gas cells," *J. Vac. Sci. Technol.* **A 10**, 2119 (1992).
12. Michael Seal, "A review of methods of bonding or making electrical contacts to diamond," *Diamond Review* **29**, 408 (1969).
13. M. Itoh, M. Hori, H. Komano, and I. Mori, *J. Vac. Sci. Technol* **B9(6)**, 3262-3265 (1991).
14. K. Suzuki, R. Kumar, H. Windischmann, H. Sano, Y. Iimura, H. Miyashita, and N. Watanabe, *J. Vac. Sci. Technol.* **B9(6)**, 3266-3269 (1991).
15. G.M. Wells, S. Palmer, and F. Cerrina, A. Purdes, and B. Gnade, *J. Vac. Sci. Technol.* **B8(6)**, 1575-1578 (1990).

END

**DATE
FILMED**

2 / 5 / 93

